

Silver Rubber-Hydrogel Nanocomposite as pH-Sensitive Prepared by Gamma Radiation: Part II

Ghobashy MM* and Elhady MA

Radiation Research of Polymer chemistry department, Egypt

ISSN: 2770-6613



***Corresponding author:**

Mohamed Mohamady Ghobashy,
Radiation Research of Polymer chemistry
department, National Center for Radiation
Research and Technology (NCRRT),
Atomic Energy Authority, Cairo, Egypt

Submission:  November 11, 2019

Published:  February 04, 2020

Volume 1 - Issue 1

How to cite this article: Ghobashy MM, Elhady MA. Silver Rubber-Hydrogel Nanocomposite as pH-Sensitive Prepared by Gamma Radiation: Part II. *Polymer Sci Peer Rev J.* 1(1).PSPRJ.000503.2020. DOI: [10.31031/PSPRJ.2020.01.000503](https://doi.org/10.31031/PSPRJ.2020.01.000503)

Copyright@ Mohamed Mohamady Ghobashy, This article is distributed under the terms of the Creative Commons Attribution 4.0 International License, which permits unrestricted use and redistribution provided that the original author and source are credited.

Abstract

Silver rubber-hydrogel (Natural Rubber Latex/poly acrylamide/poly methacrylic acid)/silver nanocomposites have been fabricated using gamma radiation techniques. The hydride mixtures of natural rubber latex(NRL) and acrylamide/methacrylic acid (AM/MAA) co-monomer dissolved in 50mL of (0.01 mol) AgNO₃ solution and irradiated at 20kGy. Gamma radiation induced combined effect, the crosslinking of NRL/AM/MAA and in situ reduction of Ag⁺ ions at ambient conditions. A silver nanoparticle (AgNPs) was embedded in crosslinking rubber-hydrogel of (NRL/PAM/PMAA) matrices, resulting in a very uniform dispersion with (30nm) diameter. The pH controlled of silver rubber-hydrogel of (NRL/ PAM/PMAA)/ Agby alternately the swelling degree of hybrid rubber-hydrogel matrices was evaluated. The effect of silver nanoparticles in-situ in (NRL/PAM/PMAA) matrices on the optical properties of composite films is studied experimentally. The (ATR-FTIR) spectrum and thermal analysis (DSC/TGA) results of the prepared rubber hydrogel showed pure one phase suggesting that there are fully miscible between rubber and hydrogel phases.

Keywords: Rubber; Hydrogel; Silver; Nanocomposites; Cross linked; Gamma radiation

Introduction

In previous paper (part I), Ghobashy et al. [1] explored the gamma synthesis of the first kind of silver rubber-hydrogel nanocomposite. During the gamma irradiating the mixture of rubber-hydrogel dissolved in silver nitrate solution, and then in situ reduction of Ag⁺ ions and crosslinked of rubber-hydrogel matrices were performed under the radiolysis of water. A remarkable and advantageous feature of nanoparticles prepared using this technique in contrast to those prepared using chemical synthesis is absence of uncontrolled by products. In this paper we used other kinds of rubber and hydrogel with keeping the silver metal. The optical property variation with pHs of the supporting rubber hydrogel matrices due to in-situ silver nanoparticles have been evaluated. Interesting effects of pHs were observed on swelling and optical properties of both silver nanoparticles inside rubber-hydrogel matrices. The noticeable main variations of optical properties of the host rubber-hydrogel matrices come from surface plasmon resonance phenomena of silver nanoparticles. The presence of silver nanoparticles embedded inside the rubber-hydrogel matrices has been confirmed by the surface plasmon resonance response (SPR) at 400-420nm. In which the particle electron cloud oscillates with the field of electromagnetic radiation. The surface plasmon resonance is dependent on the particle size ,shape and pH of surrounding environment, e.g. The net charge on the (AgNPs) is affected by pH of its surrounding environment and can become more positively or negatively charged. The pH at which the net charge zero is called the isoelectric point of (AgNPs). The decrease in the magnitude of the potential (less negative) with decreasing pH is most likely the result of decreasing OH⁻ concentration which generates a negative surface charge in alkaline pH environments [2]. The charge of the polymer chains can easily be tuned by altering the pH of the solutions with the introducing of silver particles [3].

Poly acrylamide is neutral polymer. The most frequently used flocculants are polymers derived from the acrylamide monomer [4]. Swelling equilibrium for polyacrylamide PAM -based polyampholyte hydrogels [5] and other anionic polyelectrolyte polymer such as

methacrylic acid and 1,2-dimethyl-5-vinylpyridinium methyl sulphate [6] [(methacrylamido)propyl] trimethylammonium chloride (MAPTAC) and sodium styrene sulfonate (SSS) [7] or could be crosslinked with other kind such as wax [8]. Natural Rubber Latex (NRL) is an eco-friendly latex material that comes from the bark of the rubber tree, *Hevea brasiliensis*. After collection, the latex is treated with a preservative, typically ammonia, to prevent coagulation and is transported to a processing facility for concentrating and compounding. Natural rubber Latex (NRL) which has been investigated for more than 70 years. It includes relevant properties, utilization, and potential applications [9]. It soon became evident that to find NRL formed hybrid materials. Recent advances in polymer synthesis have opened ways to prepare composite and hybrid materials [10], that are increasingly gaining attention in material science. Composite materials are traditionally made by mixing the filler into a matrix precursor formulation, which the polymers are covalently bound to inorganic substances, such as metal nanoparticles [11]. The concept is, synthetic polymers bound to rubber made by different polymerization techniques [12,13]. Gamma radiation induced reduction of silver ions in aqueous solutions containing stabilizers (usually, high-molecular-weight compounds), polymer can obtain quite stable colloidal solutions of nanoparticles of silver metal. As was established by the pulse radiolysis method, in aqueous silver salt solutions [14]. In the absence of stabilizers, the reduction of silver ions to yield nanosized metal particles unhappened due to exceed OH^\cdot . The oxidizing OH^\cdot radicals produced in radiolysis of water should be scavenged and it can be done efficiently by adding stabilizers. The use of a polymer as a stabilizer makes it possible to prepare silver nanoparticles during the radiation-induced reduction of silver ions upon gamma irradiation of AgNO_3 solutions. On the other hand, Gamma irradiation is a promising technique to fabricate a wide scale of different materials especially polymeric materials [15-19]. γ -radiation has a convenient and effective initiation method, it rapid creation of active radical sites such as H^\cdot and OH^\cdot in the water phase at room temperature could initiate the polymerization [20]. This mean throw silver reduction the polymerization take placed.

In this study, illustrate the procedure for radiation synthesis (NRL/ PAM/PMAA)/Ag are herein discussed with a focus on their pH sensitive. Silver NPs/Rubber-hydrogel, exhibit extremely high surface charge densities. Thus, pH sensitivity of the hybrid composite (NRL/PAM/PMAA) was compared for both; Ag containing and Ag-free forms, where pH controlled and alternated the swelling degree of (NRL/PAM/PMAA) and surface plasmon band of AgNPs grown composites were characterized by powdered X-ray diffraction, SEM, FTIR and UV-VIS techniques.

Experimental

Martials

The natural rubber latex (NRL) stabilized by ammonia with a total solid content of 64.5% was provided by the Tropical Crops Research Center of Zhanjiang, China. Acrylamide monomer (AM),

methyl acrylate monomer (MAA) 99% and silver nitrate (AgNO_3) was provide from Sigma-Aldrich co. another chemicals and solvent was provide commercial without further purification.

Gamma irradiation cell

Irradiation to the required doses was carried out in the cobalt-60 gamma cell facility of National Center for Radiation Research and Technology (NCRRT), Atomic Energy Authority of Egypt (AEAE), Cairo. The cobalt-60 gamma cell was made in India and the irradiation was carried out at a dose rate of 1.8kGy/h.

Determination of swelling ratio

The dried pH sensitive rubber-hydrogel of known weights was immersed in distilled water until the maximum swelling was obtained at room temperature. Then sample was weighted after removing excess water on the surface of sample with a tissue paper. This steps repeating three times, the same procedures are followed in case swelling in pH from 1 up to 11 . The swelling ratio was calculated as:

$$\text{Swelling ratio (g/g)} = \frac{(W_s - W_d)}{W_d}$$

Where W_s and W_d are the weights of wet and dry copolymer, respectively.

Puffer preparation

Swelling at various pHs individual solutions with acidic and basic pHs were prepared as following. pH 1 and 2 prepared by 0.1M of HCl (dilute 4.22917mL of 36.5 % HCl to a final volume of 500mL with distilled water), and 0.1M KCl (7.46g+ H_2O to 1 liter) pH 1 obtained by 97ml of HCl mix with 3ml of KCl and pH 2 by mix 10.6ml of HCl with 89.4ml of KCl. pH 3, 4, 5 and 6 prepared by 0.1M Citric acid: 19.21g/l (M.W.: 192.1) and 0.1M Sodium citrate dihydrate: 29.4g/l (M.W.:294.0). Mix citric acid and sodium citrate solutions in the proportions (46.5:3.5)ml for pH 3, (31:19)ml for pH 4 (20.5:29.5)ml for pH 5 and for pH 6 (7:43)ml. Mix and adjust the final volume to 100ml with deionized water to get the required pH 7,8, 9, 10 and 11 make up the following solutions; 0.1M disodium hydrogen phosphate (14.2g/l), 0.1M HCl and 0.1M NaOH (4g/l), Mix in the following proportions for pH 7 (75.6: 24.4 :0)ml, for pH 8 (95.51: 4.49 :0)ml, for pH 9 (95.50: 4.50 :0)ml for pH 10 (96.64:0 :3.36)ml and for pH 11 (96.53: 0 :34.7)ml, respectively.

Preparation of (NRL/PAM/PMAA)/Ag nanocomposites

Our scopes through two research papers (Part I,II) is development of new materials, and these could the simple way to the innovative combination of three different components (Rubber, hydrogel and metal). The structural combination of a rubber hydrogel networks with a nanoparticle (silver) for providing superior functionality to the composite material with applications in diverse fields, including catalysis, electronics, bio-sensing, drug delivery, nano-medicine, and environmental remediation. This mixing may result in a synergistic property enhancement of each component: by mutual those properties, the mechanical strength,

thermal stability, swelling behavior and biomedical activity of silver nanocomposite. These mutual benefits candidate these new materials to associate potential applications by researchers at near future. Illustrate the procedure for radiation synthesis (NRL/PAM/PMAA)/Ag are herein discussed (Figure 1). Two portions for prepared (NRL/PAM/PMAA), first one dissolving 0.5gm of AM monomer in 10ml solution of (30/70) (methanol/ bi distilled

water) followed by adds 0.5ml of meth acrylate monomer; second one add dropwise 10ml of emulsion solution of 64.5% NRL to the co-monomer (AM/MAA) solution, the two portion mix will by Severely stirring for 30min ,and then exposure to gamma irradiation at dose 20kGy. For (NRL/PAM/PMAA)/Ag was prepared by repeating the above steps with dissolved co-monomer (AM/MAA) solution in 10ml of 0.01mol L-1 AgNO₃ (1.7g).

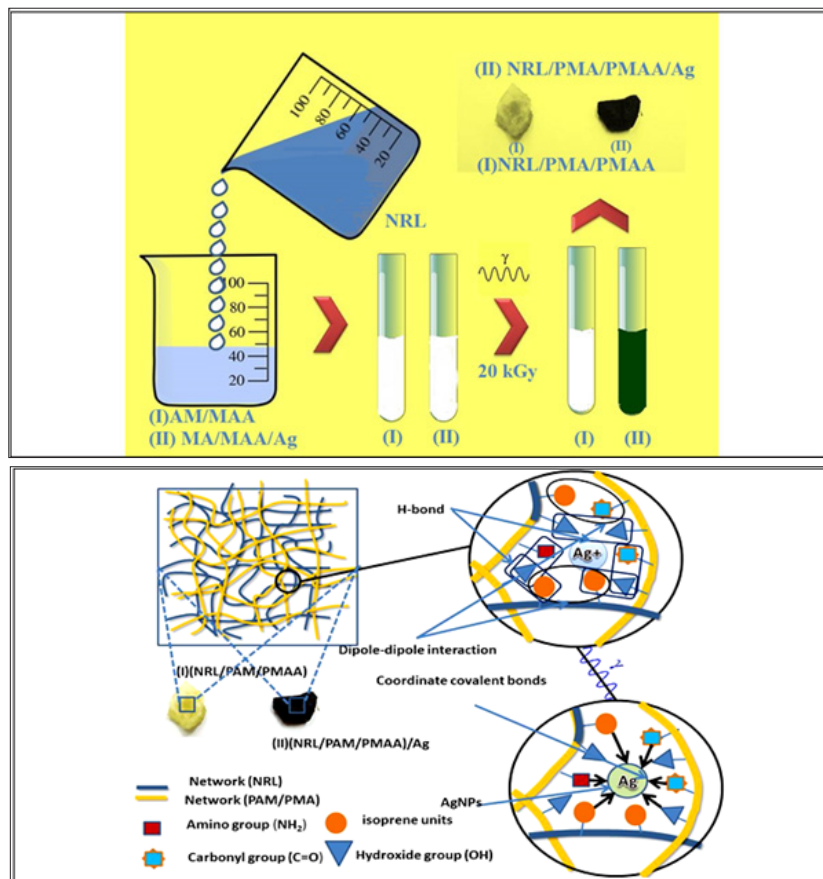


Figure 1: Demonstrating the procedure for rubber hydrogel silver nanocomposite preparation inducing by gamma irradiation and drawing the proposal embedding of silver nanoparticles composite with the two matrices of NRL rubber and PAM /PMAA hydrogel and proposal interactions between them. The silver ions reduction aided by hydrogel and radiolysis of water.

X-ray diffraction (XRD)

X-ray diffraction patterns were obtained with an XRD-6000 series, Shimadzu apparatus using Ni-filter and Cu-K α target radiation operating at 30kV and 30mA in a step scan mode with a step size of 0.02° for 2 θ and registration time of 20s per step.

Thermal analysis

Thermal analysis was measured using a DSC and TGA from TA Instruments Waters-LLC, 159 Lukens Drive, New Castle, DE 19720. the melting temperature (T_m) measured by heating the dried samples from 25 °C up to 300 °C with heating rate 10 °C/min. All measurements were conducted under a nitrogen atmosphere (20ml/min.). The cell was calibrated using an indium standard;

the weight of the sample was 5-10mg. The TGA/DTG curves were obtained with a top-loading thermo balance features; furnaces provide the highest available cooling speed. Conversely, heating from 25 C up to 600 °C with heating rate 10 °C/min under dynamic N₂ atmosphere (100ml/min.).

Fourier transforms infrared spectroscopy (ATR-FTIR)

Attenuated total reflectance-Fourier transform infrared ATR-FTIR spectroscopy Vertex 70 FTIR spectrometer equipped with HYPERION™ series microscope, BrukerOptik GmbH, Ettlingen, Germany, over the 4000- 500cm⁻¹ range, at a resolution of 4cm⁻¹. Software OPUS 6.0 (BRUKER) was used for data processing, which was baseline corrected by rubber band method with CO₂ bands excluded.

Particle size studies using transmission electron microscopy (TEM)

The particle size distribution were studied using a Transmission Electron Microscopy (TEM), JEOL JSM-100 CX, Shimadzu Co., Japan, with an acceleration voltage of 80KV. For TEM observations, the samples were prepared by making a suspension from the film

in distilled water using ultrasonic water bath. The silver rubber hydrogel samples was freezing on liquid nitrogen and quickly grind to become fine powder was suspension in acetone solution and centrifuged to separate the rubber hydrogel matrices and collimate the large size particles. Then a drop of the suspension was put into the carbon grid and left to dry at room temperature.

Results and Discussion

XRD analysis of sliver rubber-hydrogel nanocomposites

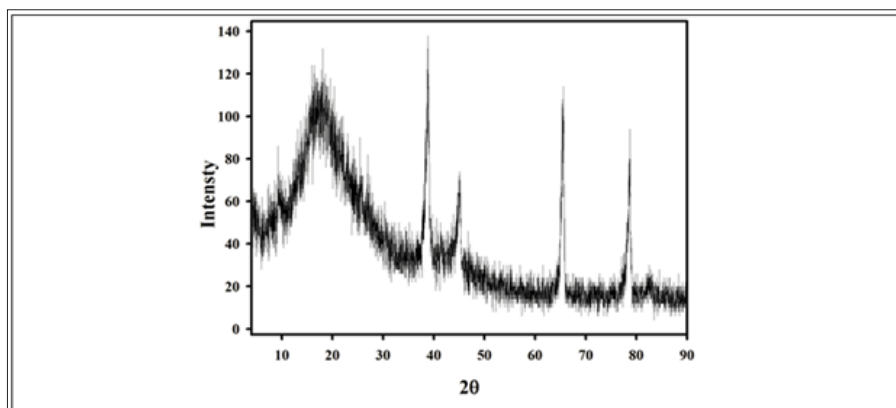


Figure 2: XRD pattern (NRL/PAM/PMAA)/Ag nanocomposites.

Figure 2 shows the XRD pattern of (NRL/PAM/PMAA)/Ag nanocomposites. The XRD shows strong and broad diffraction peak located at $2\theta=18^\circ$ due to the amorphous structure of rubber hydrogel matrix (NRL/PAM/PMAA). The X-ray diffraction pattern for silver nanoparticles in our previous literature shows four distinct diffraction peaks at 38.7° , 44.1° , 64.6° and 78.3° [silver file No. 04-0783]. These correspond to cubic, crystalline structure of silver and are assigned to (111), (200), (220) and (311) planes of silver respectively. Figure 2 shows the four characteristic peaks due to silver crystalline structure at 2θ angles of 38.80° , 45.12° , 65.60° and 78.71° corresponding to Face Centre Cubic (FCC). These values are slightly higher than those reported in JCPDS. These shifts in

peak positions of Ag towards upper angles suggested a decrease in lattice constant due to distribution of Ag nanoparticles into owing rubber-hydrogel matrix.

The crystal size of the silver nanoparticle was calculated from the line broadening using the Scherrer's formula $D = k\lambda/\beta\cos\theta$. The sizes were calculated from all the four peaks and were found to be 13nm, 12nm, 12nm and 11nm respectively. The XRD pattern indicated that the rubber-hydrogel matrix success with gamma radiation to reduction Ag^+ ions forming uniform nanoparticles Ag prevented the Ag nanoparticles from being oxidized even in air, compared with the uncoated Ag nanoparticles.

Transmission electron microscopy (TEM)

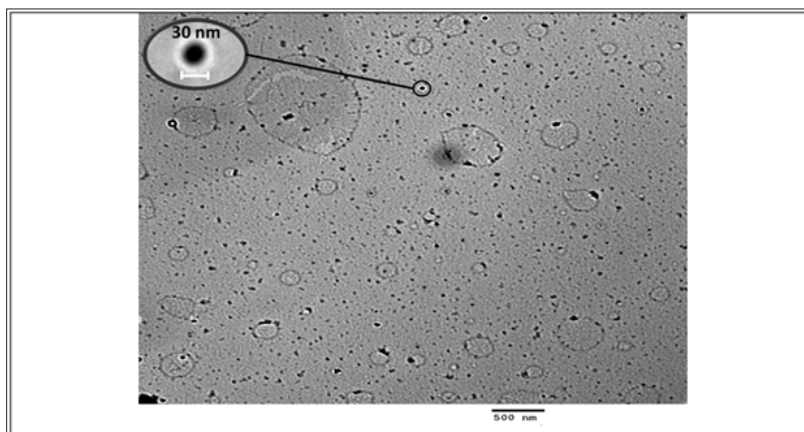


Figure 3: TEM micrographs of (NRL/PAM/PMAA)/Ag nanocomposite.

A typical TEM image is used to characterize the size, shape and morphologies of the formed silver nanoparticles. The TEM image of the silver is displayed in Figure 3. The Ag nanoparticles were readily generated during gamma irradiation. The silver nanoparticles are well distributed in the rubber-hydrogel matrices were TEM image reveals the uniform sphere structure shape of Ag nanoparticles was in the size of 30nm. This is evidence of the protection that the rubber-hydrogel matrix exerts against oxidation of the Ag core. Thus, quite stable Ag nanoparticles could be fabricated the lower size of silver nanoparticles indicated that rubber-hydrogel was employed efficiently as a reducing agent.

Swelling characterization under influence of pH

Silver NPs / Rubber-hydrogel composites in general, exhibit extremely high surface charge densities influence by pH of surrounding environmental. Thus, provide the high responsive pH. Figure 4a & 4b shown pH solution from 1 to 11 has an extremely effect on the water uptake by prepared composite after 24h has

been performed, where swelling equilibrium depend on the surface charge of the AgNPs. Figure 4a shown the effect of pH with the equilibrium swelling of (NRL/PAM/PMAA).The polyampholytes matrices of (PAM/PMAA) have both pKa, pKb for amine groups in PAM was approximately 9 [21] and/or 9.5 [22] and for PMAA is appear to be stronger acids in copolymerized with PAM than do itself pKa are less more than 3.35, where pKa's examined as a function of extent of ionization [23,24] while the charged of NRL were controlled with the pH at the isoelectric point is 2.95 [25]. Therefore at pH 1 and 2 the surface charge of NRL are positive and swelling degree were 19.3 and 18.8 (%) at pH1 and2 respectively before return decreased at pH 3 to 12 (%) and due to the pKa of PMA was more than3.35 the swelling degree has begun increased at pH 4 and 5 about 14.4 and 19.2 (%) before returned decreased at pH 6 to 13.1 (%). At pH 7 the polymer is significantly more charged in solutions of pH 7 than it is in solutions of pH 8. In the solutions with pH 7, the polymer is strongly charged and thus the absorbed water increased at pH7=18.4.

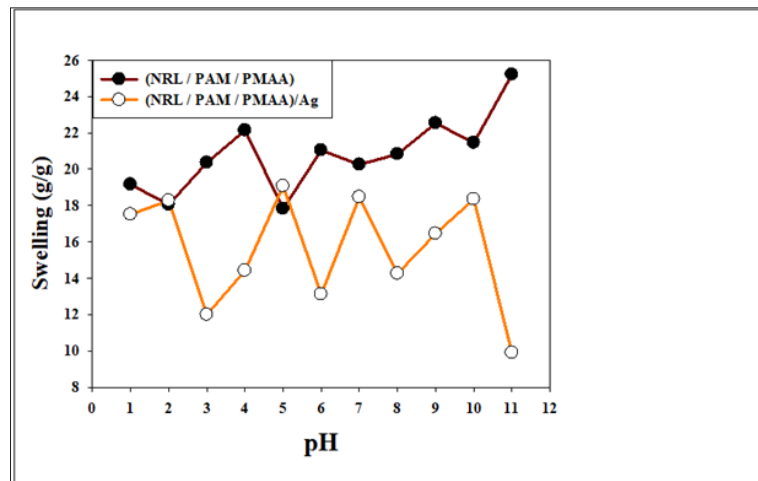


Figure 4: The swelling degree under effect of pH ranged from 1 to 11 of (a) rubber hydrogel matrix (NRL/PAM/PMAA) free Ag and (b) with AgNPs composites.

The predominant pKb value of the amine groups in the polyampholytes under consideration was approximately 9 and 9.5. Thus, swelling increased at pH values around 9-9.5, so the equilibrium swelling degree increased from pH 8 and 9 about 14.2 and 16.5, respectively as shown in Figure 4a. At pH 10 there are affective factor should consider: the NaOH leads to the hydrolysis of $-COONH_2$ groups for PAM into ionizable $-COONa$, the hydrolysis was partial and most of the $-CONH_2$ groups were not hydrolyzed completely. According to the literatures [26,27] so the amount of COO^- are increased induced electrostatic repulsion between charged groups and the rubber-hydrogels showed greater swelling=18.3 (g/g). This electrostatic repulsion at high basic solutions pH11 is prevent due to "charge screening effect" by excess Na^+ in the swelling media [28] which shield the COO^- anion groups and swelling degree return decrease at pH11 to reach about 10%. Silver NPs/Rubber -hydrogel in general, exhibit extremely high surface charge densities. Thus, provide the high responsive pH as shown in Figure 4b. The difference of the swelling ratios between

acidic and basic environment is remarkable

No significant change are recorded of swelling equilibrium at pH 2 and pH 5 maybe due to the electro neutrality points of silver surface particles charges compare to values obtained in the acidic media pH 1, pH 3 and pH 4. Due to in acidic condition where positive charge was present on the (NRL) surface and AgNPs having negative charge mainly from citrate group of buffer solution [29] able to absorb silver on the NRL surface, so the electrostatic interaction being the driving force [30]. This interaction increased at pH 3 which is the isoelectric point of NRL has more ionized charged leads to increase of swelling degree about 20.2% before return increase at pH 4 about 22.4% pH solution effected on the surface charge of the AgNPs, OH^- which generates a negative surface charge in alkaline pH environments [31]. The increased of negative charge on the AgNPs surface lead to decrease in the size of particles as shown early in UV data, increased the repulsion between particles lead to increase the network gap space, and increased the adsorbed

amount of water at pH>6 rather than free silver. Beside The iso-electric point of this polyampholyte In a pH range above 6.0 [21], where the polyampholyte are expected to be negative in net charge so the repulsion force with the negative surface charge of AgNPs take placed and the swelling moderated increased rather than the silver free. The equilibrium swelling degree increase dramatically about 5 times at pH 6 , 7, 8, 9, 10 and 11 for 21, 20.20, 20.82, 22.53, 21.44 and 25.22%, respectively.

Chemical composition detected by ATR-FTIR

The ATR-FTIR spectrum (Figure 5a) of (NRL/PAM/PMAA)/Ag showed that there is a chemical bonding between rubber hydrogel matrices and silver nanoparticles [32] .this causing shifts of main

characteristic IR band as comparison with Figure 5b showed that the stretching splitting band of (C=O) groups contracted at 1657 cm^{-1} are shifted to 1695 cm^{-1} with broadening, while no shifted was observed in the peaks attributed to C-H at 2918 cm^{-1} and abroad peaks from 3100 to 3650 cm^{-1} due to possibility formation of H-bonds between PAM and PMAA chains (NH_2 and C=O) as shown in Figure 5a, these peaks was observed in low intensity when AgNPs were introduced as shown in Figure 5b. From above results N and O atoms in the molecule of function groups have affinity for silver ions and metallic silver coordination [33,34]. This results give spot about reduction of silver nanoparticles was performance by rubber hydrogel compositions this make stabilization of silver nanoparticles.

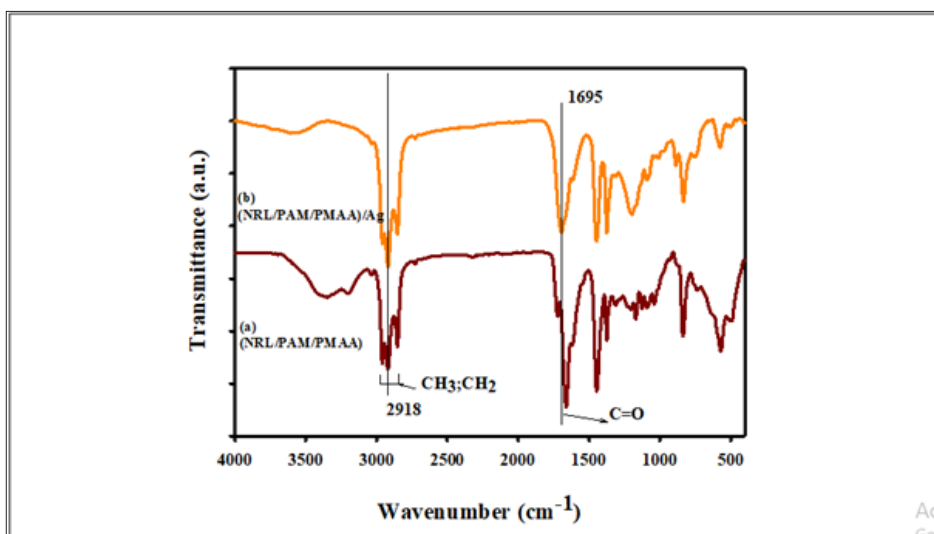


Figure 5: ATR-FTIR spectra of (a) (NRL/PAM / PMAA) and (b) (NRL/PAM/PMAA)/Ag nanocomposite

Thermal analysis of hydride rubber-hydrogel matrices with Ag nanocomposite

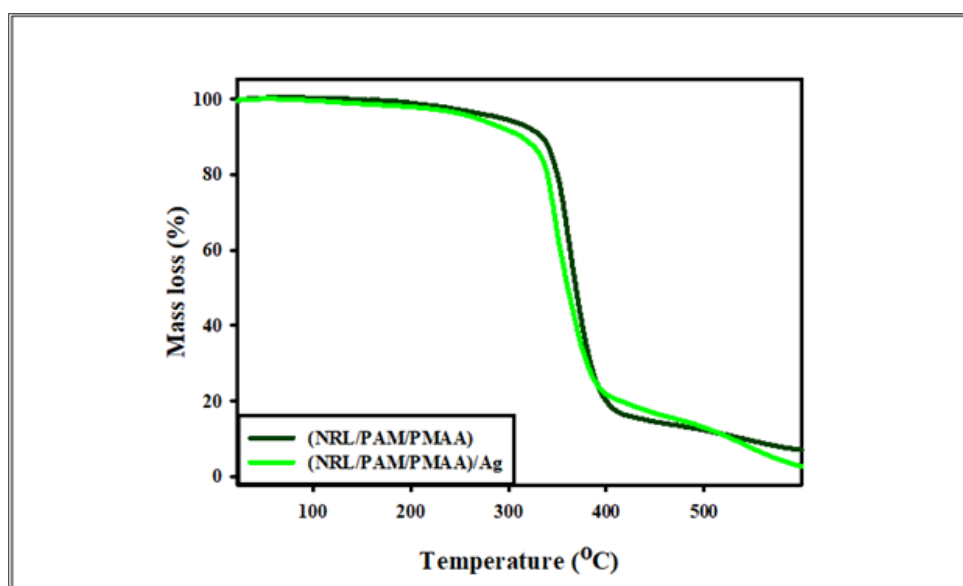


Figure 6: The TGA curve for (NRL/PAM/PMAA) and (NRL/PAM/PMAA)/Ag.

The TGA curves presented in Figure 6 shown the thermal decomposition of (NRL/PAM/PMAA) with and without AgNPs given one distinct stages of decomposition from 30 °C to 500 °C. This indicated that the miscibility of rubber NRL and copolymer hydrogel (PAM/PMAA) take place. This stage of decomposition for AgNPs free and nanocomposite with (NRL/PAM/PMAA) are coincide with varying in mass loss increased than 2% due to a small quantity of AgNPs (0.1m mol) have a less effect in the thermal stability of (NRL/PAM/PMAA) in the range from 30 °C to 500 °C, at last thermal decomposition stage (residual) from 500 °C to 600 °C the residual mass at this stage is 7.5% for (NRL/PAM/PMAA) and 2.1% for (NRL/PAM/PMAA) /Ag this attributed to the loosely bound with the remaining intermolecular H-bonds causing due to AgNPs inside the rubber-hydrogel matrices, The inclusion of AgNPs an enhancement of the degradation temperature. The DSC analysis

is one of the convenient techniques to measure the Tg and Tm. The glass transition temperature (Tg) value can provide information on how the chain mobility can be affected when adding AgNPs act as filler/matrix interactions. DSC experiments were performed for free AgNPs and (NRL/PAM/PMAA)/Ag nanocomposites. Figure 7a shows the DSC thermogram of (NRL/PAM/PMAA) with one glass temperature Tg at 58.20 °C and one endothermic Tm sharp peaks at 179.12 °C (Figure 7b). When AgNPs embedded in the rubber hydrogel matrix the Tg was decreased at 57.02 °C this due to AgNP act as filler and caused decreased in Tg of rubber hydrogel matrix [35] may be due to the AgNPs increased the crystallinity of rubber hydrogel matrix. The one sharp melting endothermic of (NRL/PAM/PMAA)/Ag was observed with shift at 191.30 °C might suggest addition of the miscibility of hydride rubber-hydrogel matrix groups.

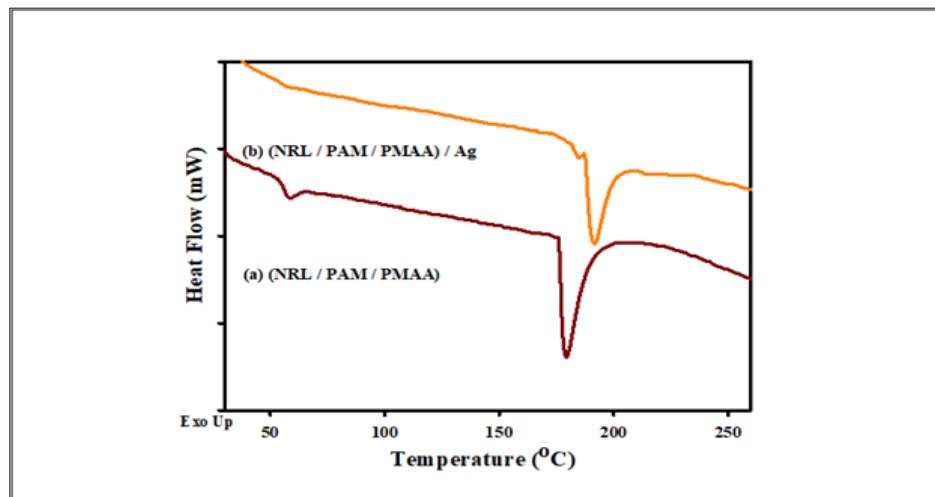


Figure 7: The DSC thermogram for (a) (NRL/PAM/PMAA) and (b) (NRL/PAM/PMAA)/Ag.

Plasmon resonance absorption of AgNP with pH change

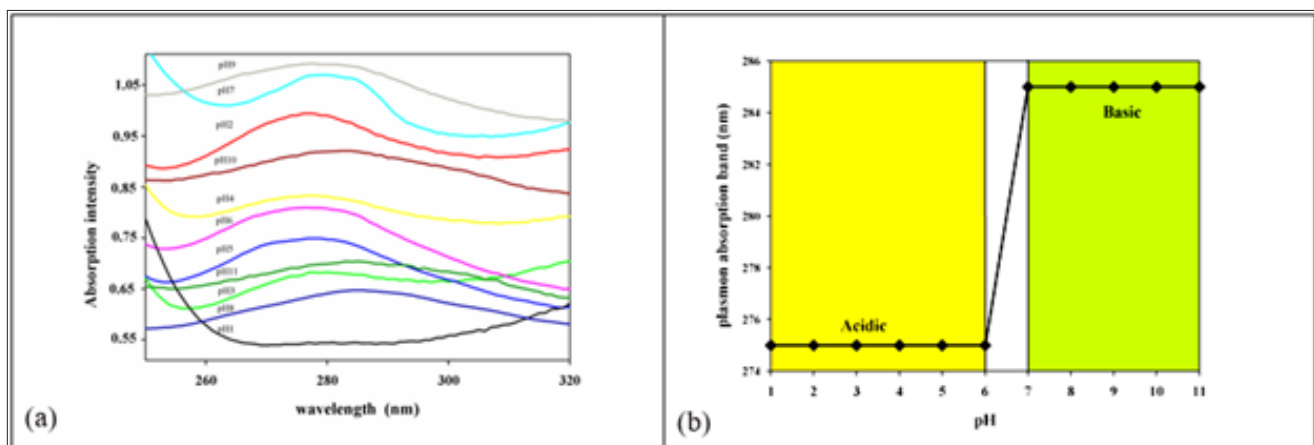


Figure 8: (a) Absorption intensity band arises from different sized silver nanoparticles with the variation of pH. (b) pH affecting on plasmon absorption band (nm) of Ag nanoparticles dispersed in rubber hydrogel matrix. The curve indicates the blue shift with pH variation from acidic to basic

The surface plasmon resonance (SPR) of silver nanoparticles (AgNPs) was studied with the differ pH. As shown in Figure 8a colloidal dispersion of (AgNPs) has absorption bands in the wavelength at 275nm attributed to AgNP clusters containing four silver atoms Ag_4^{2+} [36].The formation of the tetramer di-cation Ag_4^{2+} in solution, due to the possibility of controlling cluster sizes during the early stages of nucleation processes [37] the peak of the plasmonic band appears at 275nm with shift to 285 [38] during the change of pH process from acidic to base. This indicates that the

silver clusters are always within the different size. The increase of the absorption reflects the increasing number of such small silver particles over pH dependent. Figure 8b shown the intensity of plasmon absorption band at wavelength 275nm and 285nm with pH variation different sized silver nanoparticles has obtained. Both blue and red-shifts of the peak position are observed, depending on the presence of electron donors and/or acceptors in the solution, respectively [38]. This means that the silver in acid smallest than in base.

Demonstrate pH color sensing for (NRL/PAM/PMAA)/Ag

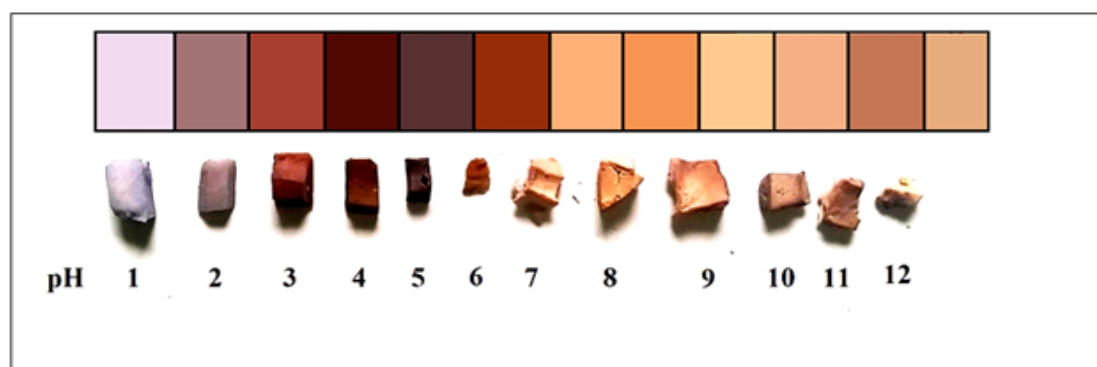


Figure 9: Monitoring colour index of (NRL/PAM/PMAA)/Ag as pH sensor

The rubber hydrogel silver (RHS) domain is presented as an appropriate candidate as pH sensor. A highly stable and accurate pH sensor for (NRL/PAM/PMAA)/Ag applications was investigated based on the potential colure change which is pH dependent. The efficacy of this new type of pH sensor has been tested using samples of (NRL/PAM/PMAA)/Ag was tested on pHs ranged from 1 up to 12 . According to (Figure 9) monitoring the index of colure varying from pH 1 to pH 12 these might be attributed to Ag-nanoparticles are responsible for the formation of localized electronic states in the Highest Occupied Molecular Orbital-Lowest Unoccupied Molecular Orbital (HOMO-LUMO) gap [39] for rubber hydrogel domains. These localized electronic states dominate the optical of real samples of (NRL/PAM/PMAA)/Ag . The role based on enhancing the electron transitions leading to the observed change in optical band gap leading to the observed change in colors.

Conclusion

Successfully prepared of pH sensitive rubber-hydrogel matrices using gamma irradiation dose at 20kGy give new materials for wide application. Silver nanoparticles (30nm) were formed in-situ reduction induced by gamma radiation resulting from water radiolysis. A silver nanoparticle was embedded into prepared rubber-hydrogel to confirm its ability for using as capping agent [40]. The DSC, TGA and SEM confirmed the one phase formation of new matrices and ATR-FTIR confirmed the formation of H-bonds between PAM and PMAA chains. Swelling measured give advised to how the rubber can swell in aqueous phases and different values of pH has been investigated. And surface plasmon resonance showed that the size of AgNPs is smallest in acid than in base medium. A

future using of (NRL/PAM/PMAA)/Ag as pH sensor need further study and extent of discussion.

References

1. Ghobashy MM, Awad A, Elhady MA, Elbarbary AM (2017) Silver rubber-hydrogel nanocomposite as pH-sensitive prepared by gamma radiation: Part I. Cogent Chemistry 3(1): 1328770
2. Badawy AME, Luxton TP, Silva RG, Scheckel KG, Suidan MT, et al. (2010) Impact of environmental conditions (pH, ionic strength, and electrolyte type) on the surface charge and aggregation of silver nanoparticles suspensions. Environ Sci Technol 44(4): 1260-1266.
3. Kacmaz S, Ertekin K, Oter O, Hizliateş CG, Ergun Y, et al. (2015) Manipulation of pH induced sensitivity of a fluorescent probe in presence of silver nanoparticles. J Lumin 168: 228-235.
4. Fevola MJ, Hester RD, McCormick CL (2003) Molecular weight control of polyacrylamide with sodium formate as a chain-transfer agent: Characterization via size exclusion chromatography/multi-angle laser light scattering and determination of chain-transfer constant. J Polym Sci Part A: Polym Chem 41(4): 560-568.
5. Baker JP, Stephens DR, Blanch HW, Prausnitz JM (1992) Swelling equilibria for acrylamide-based polyampholyte hydrogels. Macromolecules 25(7): 1955-1958.
6. Starodubtsev S, Ryabina V (1987) Swelling and collapse of polyampholyte networks of copolymers of acrylamide with methacrylic acid and 1,2-dimethyl-5-vinylpyridinium methyl sulphate. Polym Sci USSR 29(11): 2505-2511.
7. Baker JP, Blanch HW, Prausnitz JM (1995) Swelling properties of acrylamide-based ampholytic hydrogels: Comparison of experiment with theory. Polym 36(5): 1061-1069.
8. Ghobashy MM, Elhady MA (2017) pH-sensitive wax emulsion copolymerization with acrylamide hydrogel using gamma irradiation for dye removal. Radiation Physics and Chemistry 134: 47-55.

9. Patosuo T (2014) Chem Manuf Appl Nat Rubber p. 452.
10. Braunecker WA, Matyjaszewski K (2008) Basics of polymer chemistry. Prog Polym Sci 33: 165.
11. Lowe AB, Sumerlin BS, Donovan MS, McCormick CL (2002) Facile preparation of transition metal nanoparticles stabilized by well-defined (co)polymers synthesized via aqueous reversible addition-fragmentation chain transfer polymerization. J Am Chem Soc 124(39):11562-11563
12. Ali AMM, Subban RHY, Bahron H, Yahya MZA, Kamisan AS (2013) Investigation on modified natural rubber gel polymer electrolytes for lithium polymer battery. J Power Sources 244: 636-640.
13. Ramarad S, Khalid M, Ratnam C, Chuah AL, Rashmi W (2015) Rubber recycling: Challenges and developments. Prog Mater Sci 72: 100-140
14. Mostafavi M, Marigner JL, Amblard J, Belloni J (1989) Nucleation dynamics of silver aggregates simulation of photographic development processes. Radiat Phys Chem 34(4): 605-617.
15. Ghobashy MM (2017) Combined ultrasonic and gamma-irradiation to prepare TiO₂@PET-g-PAAc fabric composite for self-cleaning application Ultrasonics Sonochemistry 37: 529-535.
16. Ghobashy MM, Khozemey E (2016) Sulfonated gamma irradiated blend poly (styrene/ethylene-vinyl acetate) membrane and their electrical properties. Advances in Polymer Technology 37(5): 1249-1255.
17. Younis SA, Ghobashy MM, Mahmoud Samy (2017) Development of aminated poly(glycidyl methacrylate) nanosorbent by green gamma radiation for phenol and malathion contaminated wastewater treatment. Journal of Environmental Chemical Engineering 5(3): 2325-2336.
18. Ghobashy MM, Abdel Reheem AM, Mazied NA (2017) Ion etching induced surface patterns of blend polymer (Polyethylene Glycol-Poly Methyl Methacrylate) irradiated with gamma rays. International Polymer Processing 32(2): 174-182.
19. Ghobashy MM, Abdeen ZI (2016) Radiation crosslinking of polyurethanes: Characterization by FTIR, TGA, SEM, XRD, and Raman Spectroscopy. Journal of Polymers.
20. Ghobashy MM, Khafaga MR (2017) Chemical modification of nano polyacrylonitrile prepared by emulsion polymerization induced by gamma radiation and their use for removal of some metal ions. Journal of Polymers and the Environment 25(2): 343-348.
21. Sezaki T, Hubbe MA, Heitmann JA, Argyropoulos DS (2006) Colloidal effects of acrylamide polyampholytes. Part 1, Electrokinetic behavior. Colloids Surf A 281(1-3): 74-81.
22. Santos AM, Elaïssari A, Martinho JM, Pichot C (2005) Synthesis of cationic poly(methyl methacrylate)- poly (N-isopropyl acrylamide) core-shell latexes via two-stage emulsion copolymerization. Polym 46(4): 1181-1188.
23. Braude EA, Nachod FC (2013) Determination of organic structures by physical methods. (1st edn), Elsevier, Academic Press, Cambridge, Massachusetts, USA.
24. Wen S, Yin X, Stevenson WTK (1991) Preparation and characterization of polyelectrolyte copolymers containing methyl methacrylate and 2-hydroxyethyl methacrylate. I. polymers based on methacrylic acid. J Appl Polym Sci 42(5): 1399-1406.
25. Chaiyasat P, Suksawad C, Nuruk T, Chaiyasat A (2012) Preparation and characterization of nanocomposites of natural rubber with polystyrene and styrene-methacrylic acid copolymer nanoparticles. Express Polym Lett 6(6): 511-518.
26. Mohd Amin MCI, Ahmad N, Pandey M, JueXin C (2014) Drug Dev Ind Pharm 40: 1340.
27. Tanaka T (1981) Gels. Scientific American 244(1): 124-136.
28. Mirdarikvande S, Sadeghi H, Godarzi A, Alahyari M, Shasavari H, et al. (2015) Effect of pH, and salinity onto swelling properties of hydrogels based on H-alginate-g-poly(AMPS). Biosci Biotechnol Res Asia 11(1).
29. Agnihotri S, Mukherji S, Mukherji S (2014) Size-controlled silver nanoparticles synthesized over the range 5–100nm using the same protocol and their antibacterial efficacy. RSC Adv 4: 3974-3983
30. Chaiyasat P, Suksawad C, Nuruk T, Chaiyasat A (2012) Preparation and characterization of nanocomposites of natural rubber with polystyrene and styrene-methacrylic acid copolymer nanoparticles. Express Polym Lett 6(6): 511-518.
31. El Badawy AM, Luxton TP, Silva RG, Scheckel KG, Suidan MT, et al. (2010) Impact of environmental conditions (pH, ionic strength, and electrolyte type) on the surface charge and aggregation of silver nanoparticles suspensions. Environ Sci Technol 44(4): 1260-1266
32. Kupiec AS, Malina D, Wzorek Z, Zimowska M (2011) Influence of silver nitrate concentration on the properties of silver nanoparticles. IET Micro & Nano Lett 6(8): 656-660
33. Silvert PY, Urbina RH, Duvauchelle N, Vijayakrishnan V, Elhsissen KT (1996) Preparation of colloidal silver dispersions by the polyol process. Part 1-synthesis and characterization. J Mater Chem 6: 573-577.
34. Khanna PK, Gokhale R, Subbarao VVVS (2004) Poly(vinyl pyrrolidone) coated silver nano powder via displacement reaction. J Mater Sci 39: 3773-3776.
35. Ash B, Schadler L, Siegel R (2002) Glass transition behaviour of alumina/polymethylmethacrylate nanocomposites. Mater Lett 55(1-2): 83-87.
36. Belloni J, Amblard J, Maringer J, Mostafavi M (1994) Springer-Verlag, Heidelberg, Germany, 56: 291.
37. Michaelian K, Rendon N, Garzón IL (1999) Structure and energetics of Ni, Ag, and Au nanoclusters. Phys Rev B 60(3): 2000.
38. Smolentseva E, Gurin V, Petranovskii V (2012) Self-assembly of size-selected clusters and nanoparticles of Cu, Ag and Au in mordenite matrix. Rev Mex Ing Quim 11(3): 469
39. Mogensen KB, Kneipp K (2014) Size dependent shifts of plasmon resonance in silver nanoparticle films using controlled dissolution: Monitoring the onset of surface screening effects. J Phys Chem C 118(48): 28075-28083.
40. Ghanipour M, Dorrani D (2013) Effect of Ag-nanoparticles doped in polyvinyl alcohol on the structural and optical properties of PVA films. J of Nanomaterials.

For possible submissions Click below:

Submit Article